Cross-sectional design of sputtered aluminum nitride electro-optical phase shifters

V. Lozovski[1], W. A. P. M. Hendriks[1], L. Chang[1], D. B. Bonneville[1] and S. M. García-Blanco[1]

[1] Integrated Optical Systems Group, MESA+ Institute for Nanotechnology, University of Twente, 7500 AE Enschede, The Netherlands

Abstract

The absence of electro-optic modulators on low-loss photonic integrated circuits presents a significant challenge for applications such as photonic quantum computing, integrated ion traps, and integrated extended cavity diode lasers. The potential of aluminum nitride (AlN) electro-optical phase shifters (EOPS) lies in its broad transparency window, high breakdown voltage, immunity to parasitic charge carrier effects, and compatibility with CMOS fabrication technologies used for photonic platforms. By focusing on sputtered (polycrystalline) AlN, which enables the monolithic integration of the modulator with low-loss passive waveguides such as aluminum oxide, this study aims to optimize the electro-optic performance of highly manufacturable AlN EOPS.

Sputtered AlN has its C-axis orientation normal to the surface and reduced Pockels effect, requiring a precise cross-sectional design to ensure good performance. We simulated the influence of geometrical parameters in three different configurations on key performance metrics searching to increase the bandwidth and decrease half-wave voltage (Vπ) and waveguide propagation loss.

Although, we observe trade-offs between Vπ, bandwidth, and waveguide propagation loss across all designs, this study shows that the metric to be taken into account above all is the product $V_\pi \times L$. Optimal geometries identified in this work, as well as possible related fabrication issues, can provide guidance for future device fabrication efforts.

Introduction

Several applications like ions traps quantum computing [1], UV-VIS spectroscopy [2], [3] or microscopy require integrated high-speed modulators in the UV-VIS region. Combining Pockels effect, and very large band-gap (6.2 eV), AlN is one of the rare materials allowing GHz modulation in the UV. Moreover it can be deposited by reactive RF sputtering, offering relatively fast CMOS compatible fabrication process and making it a good competitor for lithium niobate (LN) active devices in VIS-NIR regions. However, sputtered AlN thin films, due to their polycrystalline structure, present quite low Pockels coefficients, not exciding 1 pm/V [4], [5] (compared to 30 pm/V for LN [6]) and have their c-axis orientation normal to the surface, restricting the application of the electric field in the vertical direction.

This work proposes a cross-sectional design (CSD) with optimal insertion loss (IL) and V_π in DC regime, for two distinct configurations of lumped electrodes. In this work, the design wavelength is 1550 nm, which allows an easier experimental validation. UV wavelength designs will follow in the future.

1) Simulation setup

Evenly for phase or intensity modulation, the maximal resulting phase-shift must be $\Delta\phi = \pi$, achieved for a driving voltage $V_0 = V_\pi$, called the half-wave voltage [7]: $V_\pi = \frac{\lambda Re\{n_{eff}\}g}{Lr_{ij}n_{core}^4\Gamma}$ (1), where $\Gamma = \frac{\iint_{AlN}|E_{x,y}|^2.E_z dxdy}{\iint_{-\infty}^{+\infty}|E_{x,y}|^2 dxdy}\frac{g}{V}$ is the overlap between the RF electric field and the mode, g is the gap between electrodes, $r_{ij} = \{r_{13}, r_{33}\}$ is the Pockels coefficient (for TE or TM modes respectively) and $n_{core} = \{n_o, n_e\}$ refractive index of the core (for TE or TM modes respectively). To suppress the dependance of V_π on L we introduce a figure of merit, constant for a certain CSD, that denotes the electro-optical conversion efficiency: $V_\pi . L = V . L_\pi = \frac{\lambda n_{eff} g}{r_{ij} n_{core}^4 \Gamma}$. One can notice that reducing $V_\pi L$ product contributes to the reduction of total losses. It is a good reason to mention another figure of merit: $V_\pi L \times \alpha$, physically representing the total device loss for $V_\pi = 1$ V.

"Electrostatics" and "Electromagnetic Waves, Frequency Domain" simulation modules of COMSOL Multiphysics were used to evaluate and compare two CSD configurations. The structure cross section and the corresponding fundamental TE optical mode is shown in Figure 1.

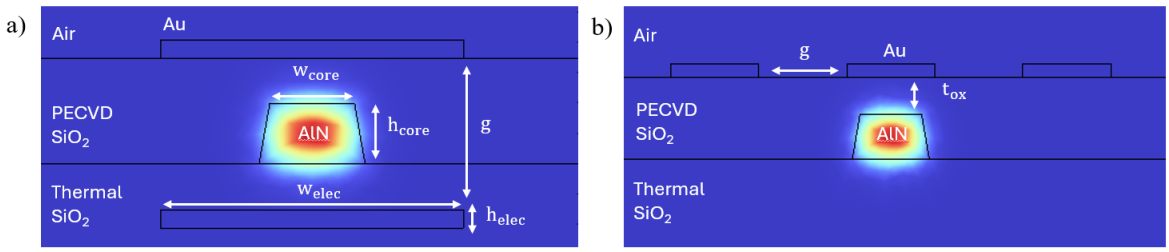

Figure 1: a) and b) show Configurations 1 and 2 of CSD.

We propose to test two configurations most commonly found in the literature [8] for Z-cut crystals. All the simulations were performed with a waveguide sidewall angle of 80° for $\lambda = 1550$ nm. The $V_\pi L$ product was evaluated using formula (1) by calculating L for $V_\pi = 1$ V. Later when searching for multi-objective optimal values, we will fix $V_0 = 15$ V, closer to real case scenario.

2) Results and discussion

Progressive precision parameter sweeps were performed, with intermediate reduction of degrees of freedom.

Particularly in Configuration 2 the minimal value of g is limited by the breakdown field of the air $E_{BD,air} = 3$ V/µm, and depends on the voltage applied. If we set $V_0 = 15$ V, the lowest accessible g for Configuration 2 is $g_{min} = 5$ µm.

After reducing most of the degrees of freedom we end up with: $\{h_{core} = 1$ µm; $h_{elec} = 0.3$ µm; $w_{elec} = 5$ µm$\}$, for Configuration 1, and $\{h_{core} = 1$ µm; $h_{elec} = 0.3$ µm; $w_{elec} =$

2 µm, $g = 5$ µm}, for Configuration 2. The variations of $V_\pi L$ and $V_\pi L\alpha$ as function of $\{g, w_{core}\}$ for Configuration 1, and $\{t_{ox}, w_{core}\}$ for Configuration 2, are presented in Figure 2.

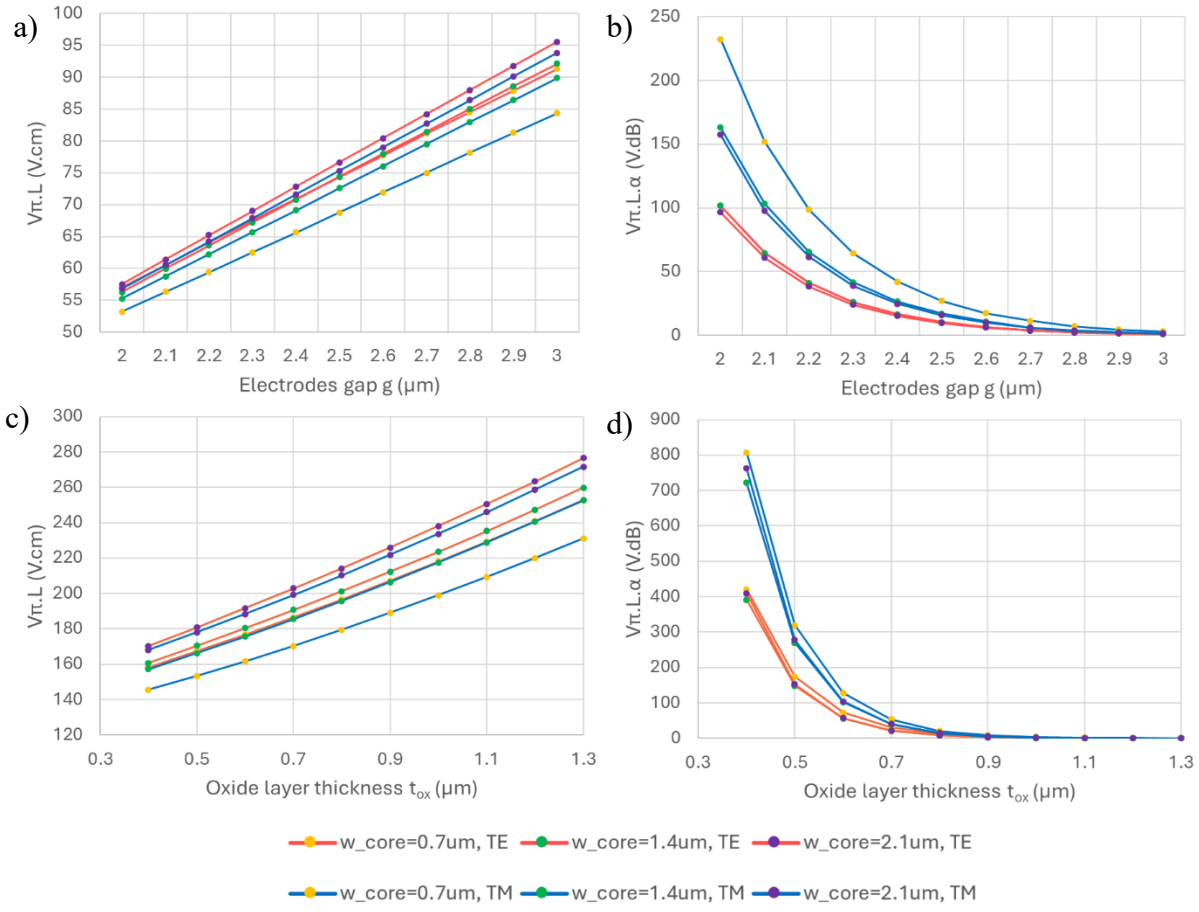

Figure 2: $V_\pi L$ (left) and $V_\pi L\alpha$ (right) as function of electrodes gap for different core width, for Configuration (top) 1 and 2 (bottom)

Finding an optimal value between $V_\pi L$ and IL can be done by searching for the minimum of the objective function: $F = \frac{|f_1 - f_{1,target}|}{f_{1,target}} + \frac{|f_2 - f_{2,target}|}{f_{2,target}}$, where f_1 is $L_\pi(V_0 = 15V)$ and f_2 is IL (total loss per device: $\alpha \times L_\pi(V_0 = 15V)$). The tested target values were: $f_1 = \{5\text{ cm}; 5\text{ mm}\}$ and $f_2 = 1$ dB.

	Targets	Values	TE or TM	Parameters (in µm)
Configuration 1	$f_1 = 5$ cm $f_2 = 1$ dB	$L_\pi = 4.97$ cm $\alpha L_\pi = 0.98$ dB	TM	$w_{core} = 0.6$ $g = 2.7$
	$f_1 = 5$ mm $f_2 = 1$ dB	$L_\pi = 4.7$ cm $\alpha L_\pi = 1.3$ dB	TE	$w_{core} = 1.3$ $g = 2.4$
Configuration 2	$f_1 = 5$ cm $f_2 = 1$ dB	$L_\pi = 12.4$ cm $\alpha L_\pi = 1.1$ dB	TM	$w_{core} = 1$ $t_{ox} = 0.8$
	$f_1 = 5$ mm $f_2 = 1$ dB	$L_\pi = 12$ cm $\alpha L_\pi = 1.3$ dB	TM	$w_{core} = 0.7$ $t_{ox} = 0.8$

Table 2: Length and IL values related to the minimum of F, and corresponding geometrical parameters, for different targets and different configurations

As expected, Configuration 1 provides the best results, but presents significant fabrication obstacles, such as sputtering chamber pollution or degradation of electrodes, due to a metallic layer under the waveguide layer. One can notice, that putting a stricter requirement on L_π does not significantly improve it, but lead to worse IL. TM modes generally perform better than TE, most certainly due to higher experienced refractive index ($n_e > n_o$). Interestingly, in most of the cases $w_{core} < h_{core}$, because counter-intuitively increasing w_{core} decreases $\frac{\iint_{core} |E_y| dS}{S_{core}}$. For Configurations 2, electrodes can be cladded with SiO_2, $E_{BD,SiO_2} > 1\ kV/\mu m$ to reduce g even more, and reach $L_\pi \approx 9\ cm$. For Configuration 1, we obtain $V_\pi L = 75\ V.cm$ which is a good result for AlN; indeed if we had $r_{33} = 30\ pm/V$, as for LN, the product would be $V_\pi L = 2.5\ V.cm$! Nonetheless, the resulting lengths of the devices might seems too high, which suggests working with folded [1] or resonant structures (ex: ring resonators).

Conclusion

Low $V_\pi L$ is an important advantage for Pockels effect modulators, and can reduce the length of the device and thus total loss (and increase the bandwidth). Simulations performed in this work showed optimal CSDs, that minimize both $V_\pi L$ and IL, for two studied configurations. A $V_\pi L$ product of 75 V.cm was achieved, for a loss of 1 dB per device, which are quite good results considering low Pockels coefficient used. These findings can be useful for an efficient electro-optical characterization of AlN thin films. Nevertheless, the devices would probably need to have folded or resonant structures to reduce the footprint or/and enhance electro-optical efficiency. Further, bandwidth, extinction ratio, scattering loss, wavelength variations, and specific consideration for each structure (Mach-Zehnder or Ring modulator) and electrical driving schemes (lumped or travelling-wave electrodes) should be included.

[1] C. W. Hogle *et al.*, "High-fidelity trapped-ion qubit operations with scalable photonic modulators," *Npj Quantum Inf.*, vol. 9, no. 1, pp. 1–6, Jul. 2023, doi: 10.1038/s41534-023-00737-1.

[2] G. Finco *et al.*, "Monolithic thin-film lithium niobate broadband spectrometer with one nanometre resolution," *Nat. Commun.*, vol. 15, no. 1, p. 2330, Mar. 2024, doi: 10.1038/s41467-024-46512-4.

[3] M. Montesinos-Ballester *et al.*, "On-chip Fourier-transform spectrometer based on spatial heterodyning tuned by thermo-optic effect," *Sci. Rep.*, vol. 9, no. 1, p. 14633, Oct. 2019, doi: 10.1038/s41598-019-50947-x.

[4] P. Gräupner, J. C. Pommier, A. Cachard, and J. L. Coutaz, "Electro-optical effect in aluminum nitride waveguides," *J. Appl. Phys.*, vol. 71, no. 9, pp. 4136–4139, May 1992, doi: 10.1063/1.350844.

[5] E. Dogheche, D. Rémiens, A. Boudrioua, and J. C. Loulergue, "Growth and optical characterization of aluminum nitride thin films deposited on silicon by radio-frequency sputtering," *Appl. Phys. Lett.*, vol. 74, no. 9, pp. 1209–1211, Mar. 1999, doi: 10.1063/1.123501.

[6] D. Zhu *et al.*, "Integrated photonics on thin-film lithium niobate," *Adv. Opt. Photonics*, vol. 13, no. 2, p. 242, Jun. 2021, doi: 10.1364/AOP.411024.

[7] X. Liu, A. W. Bruch, and Hong. X. Tang, "Aluminum nitride photonic integrated circuits: from piezo-optomechanics to nonlinear optics," *Adv. Opt. Photonics*, vol. 15, no. 1, p. 236, Mar. 2023, doi: 10.1364/AOP.479017.

[8] M. Zhang, C. Wang, P. Kharel, D. Zhu, and M. Lončar, "Integrated lithium niobate electro-optic modulators: when performance meets scalability," *Optica*, vol. 8, no. 5, p. 652, May 2021, doi: 10.1364/OPTICA.415762.